Inorganica Chimica Acta, 111 (1986) 149–155

Synthesis and Structure of an Oxidation Product of Hemiporphyrazinatoiron(II): Monoaquo-μ-oxo-bis(hemiporphyrazinato)iron(III). A Linear μ-Oxo Dimer Containing Six- and Five-Coordinated Iron Atoms

INES COLLAMATI*, GIULIA DESSY and VINCENZO FARES*

Istituto di Teoria e Struttura Elettronica e Comportamento Spettrochimico dei Composti di Coordinazione del CNR, P.O. Box 10, 00016 Monterotondo Stazione, Rome, Italy

Received May 20, 1985

Abstract

The interaction between dioxygen and wet N-base solutions of Fe(II) hemiporphyrazine (Fehp) leads to the title compound, which is a high-spin antiferromagnetically coupled iron(III) complex. The crystal and molecular structure has been determined by X-rays. The unit cell is the tetragonal space group $P4/ncc$, with $a = b = 19.083(5)$ and $c = 23.509(5)$ Å. 2141 unique observed reflections were used in the analysis, and the final conventional R is 0.059. The structure consists of Fe(III)hp μ-oxo dimers having strictly linear Fe–O–Fe units and a nearly eclipsed internal configuration. This is the first observation of the formation of a mono-adduct in a μ-oxo dimer via axial coordination of a H_2O molecule. The resulting asymmetric dimer, H_2O–FeAhp–O–FeBhp contains a six-coordinated Fe atom (FeA) lying in the plane of the four Ns of the macrocycle. The second Fe atom (FeB) is five-coordinated and lies outside of the coordination plane by 0.45 Å. The Fe–O distances are: FeA–O = 1.782(7) Å and FeB–O = 1.739(7) Å. The axial coordination of the water (FeA–O_w = 2.210(9) Å) seems weak, probably due to the labilising *trans* influence of the μ-oxo ligand. The dimers are paired coaxially to form tetramers, which are in turn connected via a two-dimensional net of hydrogen bonds. The structural results are correlated with spectroscopic, thermogravimetric and magnetic properties.

Introduction

We recently described some complexes of Fe(II) with the divalent macrocycle hemiporphyrazine (hpH_2) and the interaction of one such complex, Fe(II)hp, with O_2 in anhydrous γ-picoline [1]. If the Fe(II)hp solutions are concentrated and the solvent is not anhydrous, bubbling in O_2 leads to separation of a solid which appears to be a μ-oxo hydrate on the basis of spectroscopic and magnetic measurements.

Another example of a μ-oxo-Fe–hemiporphyrazinate, the polymer $(FehpO)_n$, has been described [2]. It appeared of interest to investigate the structure of this new μ-oxo compound and its interaction with H_2O. Crystals of diffraction quality were obtained and the crystal structure was solved. The compound is a linear μ-oxo Fe(III) dimer in which the two Fehp bridged units are non-equivalent, one of the units having a coordinated H_2O molecule: hpFe–O–FehpOH_2.

Experimental

Preparation of the Compound

The first samples were obtained as a brown microcrystalline precipitate by bubbling O_2 at room temperature (r.t.) into a solution of Fe(II)hp [1] (5×10^{-3} mol dm^{-3}) in a reagent grade, *i.e.* non-anhydrous γ-picoline. The IR spectrum of the complex shows the characteristic peaks of the Mhp core and a strong sharp band at 878 cm^{-1}, together with two broad absorptions in the ν_{OH} region centered at 3400 and 3200 cm^{-1}.

The same product was obtained from Fe(II)hp by air oxidation. Suspensions of Fe(II)hp in γ-picoline, py, or DMF* were stirred at room temperature for times varying from 24 to 48 h. The suspensions were filtered and the products washed with toluene and MeOH. Crystals were obtained by leaving the hot mother liquors to cool slowly in air for *ca.* 2 days. The compound separated as very thin needles. Elemental (CHNO) and TG analyses carried out on several samples having identical X-ray powder patterns gave a variable water content: wt. loss between 130 and 150 °C 2.0–3.5% (calc. for H_2O/[$(Fehp)_2O$]H_2O = 1.76%).

Crystals for X-ray analysis were difficult to grow. Success was achieved only after submitting suspen-

*Authors to whom correspondence should be addressed.

*Abbreviations used: py, pyridine, γ-pic, 4-methylpyridine DMF = dimethylformamide; NB = nitrobenzene; Ct, the center of hemiporphyrazinato core.

0020-1693/86/$3.50

© Elsevier Sequoia/Printed in Switzerland

sions of the μ-oxo-hydrate in wet nitrobenzene to controlled heating/cooling cycles in pyrex tubes closed under vacuum.**

The crystals had a prismatic habit, and successful refinement of the structure showed them to be of formula $[(Fehp)_2O]H_2O$ with further clathrated H_2O (H_2O:(Fehp) = 1:4).

Physical Measurements

IR spectra, thermal analyses, and magnetic measurements were performed as reported previously [3, 4].

Crystal Data

$[C_{52}H_{30}Fe_2N_{16}O_2]\cdot 0.5H_2O$ (M = 1031.616) crystallises as deep violet tetragonal prisms belonging to the space group $P4/ncc$ with the unit-cell dimensions $a = b = 19.083(5)$, $c = 23.509(5)$ Å, U = 8561 Å^3, $D_c = 1.60$ g cm^{-3}, $D_m = 1.61$ g cm^{-3} $Z = 8$, $F(000) = 4288$, Mo K_α radiation $\lambda = 0.71069$ Å, graphite monochromator, μ(Mo K_α) = 11.81 cm^{-1}.

X-ray Data Collection

A crystal of dimensions 0.4 × 0.2 × 0.1 mm was used for the data collection on a Nicolet automated four circle diffractometer. The unit-cell dimensions were obtained by least-squares refinement of setting angles for 15 reflections with $2\vartheta > 25°$. The intensities of 2141 independent reflections with $I \geq 2\sigma(I)$, recorded by the ϑ–2ϑ scan technique, were used for structure determination via Patterson and Fourier methods and for the refinement. The data were corrected for background and for Lorentz and polarization effects. No correction was applied for absorption, in view of the small crystal size and absorption coefficient.

Solution and Refinement of the Structure

Inspection of the intensity data revealed the following systematic absences consistent with the space group $P4/ncc$: $hk0$, $h + k = 2n$; $0kl$, $l = 2n$; and hhl, $l = 2n$. Two independent iron atoms were located by the heavy-atom method on the two-fold axis at $x\,x\,1/4$. The positions of the non-hydrogen atoms of the hemiporphyrazine macrocycles were found by Fourier synthesis. Successive-difference Fourier calculations gave the positions of the bridging oxygen atom and of the coordinated water molecule. The positions and the isotropic temperature parameters of the atoms were refined by a full-matrix least squares method to an R value of 0.08. The weighting scheme used throughout the refinement was $w = 1/(\sigma^2(F_o) + 0.0029\,F_o^2)$.

**The same procedure cannot be used for suspensions of the μ-oxo hydrate in DMF or in nitrogen bases such as γ-picoline. The iron(III) is reduced to iron(II), giving Fe(II)-hp·H_2O (from DMF) and Fe(II)hp(γ-pic)$_2$ (from γ-pic).

A final-difference Fourier synthesis showed the presence of a water molecule of crystallisation on the tetragonal axis at 1/4 1/4 z. All hydrogen atoms, except those belonging to the water molecules, were included at fixed calculated positions with an isotropic temperature factor of 5.0 Å^2. The refinement was continued using anisotropic thermal parameters for all non-hydrogen atoms except the oxygen atom of the crystallisation water molecule, which retained an isotropic temperature factor. The final R-value was 0.059. Atomic scattering factors and the corrections for real dispersion (iron atoms only) were taken from ref. 5.

Calculations were carried out on the IBM 3330/168 of CNUCE-CNR (Pisa, Italy) by using the SHELX Program system [6]. Figure 1 shows a diagram of the hemiporphyrazinato core. Final atomic coordinates and their standard deviations are listed in Table I and bond distances and angles in Table II. Observed and calculated structural factors and thermal parameters are listed in Supplementary Publication n.

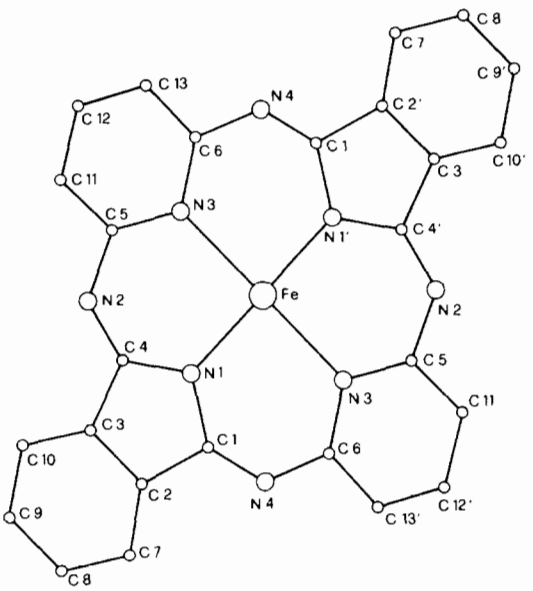

Fig. 1. Scheme of the hemiporphyrazinato iron(III) core with the labelling of the atoms.

Results

Figure 2 gives the IR spectra of $[(Fehp)_2O]\cdot H_2O$ and Fe(II)hp·H_2O [1]. Inspection shows the following significant differences: (i) A band is present at 878 cm^{-1} in the μ-oxo compound, assignable to Fe–O–Fe (asymm), which is absent in the Fe(II) compound; (ii) The ν_{OH} region is different: in Fe(II)hp·H_2O the absorption due to coordinated H_2O is centred at 3100 cm^{-1}, whereas in the Fe(III)

TABLE I. Fractional Atomic Parameters for $[(Fehp)_2O]\cdot H_2O$

	x/a	*y/b*	*z/c*		*x/a*	*y/b*	*z/c*
FeA	−0.0400(1)	0.0400	0.2500	FeB	−0.1704(1)	0.1704(1)	0.2500
OW	0.0420(3)	−0.0420(3)	0.2500	Ox	−0.1060(3)	0.1060(3)	0.2500
N1A	−0.0863(5)	−0.0187(5)	0.1910(4)	N1B	−0.2351(5)	0.1455(4)	0.1872(3)
N2A	−0.1668(5)	−0.0861(5)	0.2498(5)	N2B	−0.3126(5)	0.0652(5)	0.2335(3)
N3A	−0.0923(5)	−0.0219(5)	0.3168(4)	N3B	−0.2435(5)	0.1189(4)	0.3077(3)
N4A	−0.0456(5)	0.0405(6)	0.1061(4)	N4B	−0.1741(5)	0.1974(4)	0.1073(3)
C1A	−0.0872(7)	0.0023(7)	0.1334(5)	C1B	−0.2256(6)	0.1636(6)	0.1299(4)
C2A	−0.1507(7)	−0.0305(7)	0.1065(5)	C2B	−0.2835(5)	0.1323(5)	0.0966(4)
C3A	−0.1864(6)	−0.0676(7)	0.1485(5)	C3B	−0.3239(5)	0.0940(5)	0.1334(4)
C4A	−0.1458(7)	−0.0590(7)	0.2028(6)	C4B	−0.2913(5)	0.0994(5)	0.1900(4)
C5A	−0.1380(6)	−0.0758(6)	0.3039(5)	C5B	−0.2841(5)	0.0665(6)	0.2879(5)
C6A	−0.0776(6)	−0.0117(6)	0.3735(6)	C6B	−0.2303(5)	0.1203(6)	0.3661(4)
C7A	−0.1762(7)	−0.0262(7)	0.0518(6)	C7B	−0.2997(6)	0.1370(6)	0.0388(4)
C8A	−0.2394(8)	−0.0627(8)	0.0398(6)	C8B	−0.3593(6)	0.1012(6)	0.0215(5)
C9A	−0.2738(7)	−0.0999(9)	0.0818(6)	C9B	−0.4000(6)	0.0610(6)	0.0585(5)
C10A	−0.2469(8)	−0.1037(7)	0.1386(5)	C10B	−0.3826(5)	0.0566(6)	0.1149(4)
C11A	−0.1633(7)	−0.1221(7)	0.3486(6)	C11B	−0.3045(6)	0.0109(6)	0.3225(4)
C12A	−0.1440(7)	−0.1120(7)	0.4013(6)	C12B	−0.2865(6)	0.0106(6)	0.3784(5)
C13A	−0.1011(6)	−0.0564(6)	0.4150(5)	C13B	−0.2496(6)	0.0652(5)	0.4003(4)
OCW	0.2500	0.2500	0.2524(19)				

TABLE II. Interatomic Distances (Å) and Angles (°) with e.s.d.s in Parentheses for $[(Fehp)_2O]\cdot H_2O$

FeA–N1A	1.990(10)	FeB–N1B	1.981(8)
FeA–N3A	2.205(11)	FeB–N3B	2.180(8)
FeA–Ox	1.782(6)	FeB–Ox	1.739(6)
FeA–Ow	2.212(6)	N1B–C1B	1.404(12)
N1A–C1A	1.412(16)	N1B–C4B	1.388(13)
N1A–C4A	1.398(16)	N2B–C4B	1.278(13)
N2A–C4A	1.283(17)	N2B–C5B	1.390(13)
N2A–C5A	1.400(17)	N3B–C5B	1.346(13)
N3A–C5A	1.382(15)	N3B–C6B	1.396(11)
N3A–C6A	1.374(17)	N4B–C1B	1.289(13)
N4A–C1A	1.255(17)	N4B–C6B	1.357(14)
N4A–C6A	1.388(17)	C1B–C2B	1.479(14)
C1A–C2A	1.502(19)	C2B–C3B	1.369(14)
C2A–C3A	1.393(18)	C2B–C7B	1.398(14)
C2A–C7A	1.378(18)	C3B–C4B	1.474(14)
C3A–C4A	1.502(18)	C3B–C10B	1.399(15)
C3A–C10A	1.365(20)	C5B–C11B	1.392(15)
C5A–C11A	1.376(17)	C6B–C13B	1.375(14)
C6A–C13A	1.370(18)	C7B–C8B	1.388(16)
C7A–C8A	1.422(21)	C8B–C9B	1.396(16)
C8A–C9A	1.382(21)	C9B–C10B	1.368(15)
C9A–C10A	1.431(20)	C11B–C12B	1.359(15)
C11A–C12A	1.415(19)	C12B–C13B	1.359(16)
C12A–C13A	1.378(18)		
N1A–FeA–N'1A	170.4(4)	N1B–FeB–N'1B	148.6(4)
N1A–FeA–N3A	89.7(4)	N1B–FeB–N3B	87.5(3)
N1A–FeA–N'3A	89.8(4)	N1B–FeB–N'3B	88.3(3)
N3A–FeA–N'3A	173.3(4)	N3B–FeB–N'3B	164.6(4)
N1A–FeA–Ox	94.8(3)	N1B–FeB–Ox	105.7(3)
N3A–FeA–Ox	93.4(3)	N3B–FeB–Ox	97.7(3)
N1A–FeA–Ow	85.2(3)	FeB–N1B–C4B	126.7(6)
N3A–FeA–Ow	86.6(3)	C1B–N1B–C4B	107.6(8)

(continued overleaf)

TABLE II *(continued)*

FeA–N1A–C4A	122.1(8)	C4B–N2B–C5B	126.9(9)
C1A–N1A–C4A	109.6(10)	FeB–N3B–C5B	119.1(7)
C4A–N2A–C5A	127.0(10)		
FeA–N3A–C5A	121.8(7)	FeB–N3B–C6B	119.2(7)
FeA–N3A–C6A	121.5(8)	C6B–N3B–C5B	117.3(9)
C5A–N3A–C6A	116.6(10)	C1B–N4B–C'6B	128.2(8)
C1A–N4A–C'6A	128.2(11)	N1B–C1B–N4B	128.1(9)
N1A–C1A–N4A	130.3(12)	N1B–C1B–C2B	108.1(9)
N1A–C1A–C2A	107.2(11)	N4B–C1B–C2B	123.6(9)
N4A–C1A–C2A	122.5(11)	C1B–C2B–C3B	107.6(8)
C1A–C2A–C3A	107.9(11)	C1B–C2B–C7B	130.8(9)
C1A–C2A–C7A	130.8(12)	C3B–C2B–C7B	121.6(9)
C3A–C2A–C7A	121.3(12)	C2B–C3B–C4B	107.2(9)
C2A–C3A–C4A	107.1(11)	C2B–C3B–C10B	121.8(9)
C2A–C3A–C10A	123.3(12)	C4B–C3B–C10B	130.2(9)
C4A–C3A–C10A	129.5(12)	N1B–C4B–N2B	127.4(9)
		N1B–C4A–C3B	109.1(9)
N1A–C4A–N2A	130.2(12)	N2B–C4B–C3B	123.5(9)
N1A–C4A–C3A	108.1(11)	N2B–C5B–N3B	123.8(9)
N2A–C4A–C3A	121.7(11)	N2B–C5B–C11B	114.4(9)
N2A–C5A–N3A	123.6(10)	N3B–C5B–C11B	121.7(10)
N2A–C5A–C11A	113.0(10)	N3B–C6B–N4B	123.5(8)
N3A–C5A–C11A	123.3(11)	N3B–C6B–C13B	120.8(9)
N3A–C6A–N4A	123.4(10)	N4B–C6B–C13B	116.4(7)
N3A–C6A–C13A	122.3(11)	C2B–C7B–C8B	115.8(10)
N4A–C6A–C13A	115.6(11)	C7B–C8B–C9B	123.0(10)
C2A–C7A–C8A	117.1(12)	C8B–C9B–C10B	120.2(10)
C7A–C8A–C9A	120.8(13)	C3B–C10B–C9B	117.7(10)
C8A–C9A–C10A	121.5(14)	C5B–C11B–C12B	119.8(11)
C3A–C10A–C9A	115.9(13)	C5B–C12B–C13B	119.7(11)
C5A–C11A–C12A	118.2(12)	C6B–C13B–C12B	120.2(9)
C11A–C12A–C13A	118.8(12)		
C6A–C13A–C12A	120.5(12)		

μ-oxo dimer two absorptions are found at 3400 and 3200 cm^{-1}, probably due to the presence of two kinds of H_2O molecules, coordinated and clathrated; the lower energy value is assignable to the coordinated H_2O. (iii) There is a parallel difference in thermal stability: the water is removed from Fe(II)hp·H_2O at *ca.* 250 °C, and from the μ-oxo dimer at between 130–150 °C.

The magnetic behaviour was examined at room temperature and 85 K: μ_{eff} = 2.09 BM (r.t.) and 1.48 BM (85 K).

Description of the Structure

The structure consists of binuclear units lying on the two-fold axis passing through $\bar{x}$ x 1/4, as shown in Fig. 3. The two atoms FeA and FeB are bonded by the bridging oxygen O_x which also lies on the two-fold axis. The Fe–O_x–Fe moiety is thus exactly linear, which is not the case in the other μ-oxoiron hemiporphyrazinate $(FeOhp)_n$ (Fe–O–Fe = 158–170° [2]) and in μ-oxo Fe(III) porphyrinates (Fe–O–Fe 172.5–178.5° [7]). The two hemiporphyrazine units are superposed in parallel, the separation between the planes of the coordinated nitrogens being 3.97 Å. The mutual rotation of the two planes about the Fe–O–Fe direction is 6°.

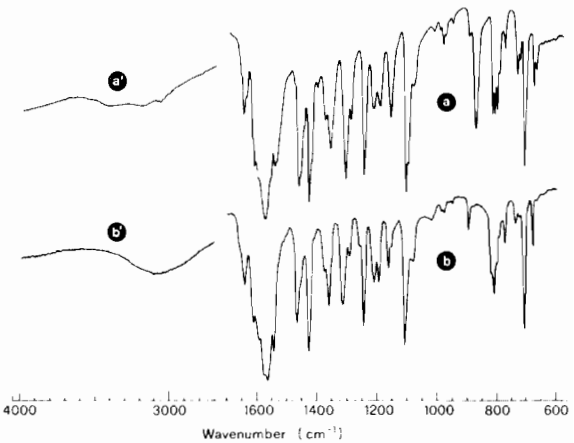

Fig. 2. IR spectra (nujol mulls) of: (a) $[(Fehp)_2O]\cdot H_2O$, (b) Fe(II)hp·H_2O.

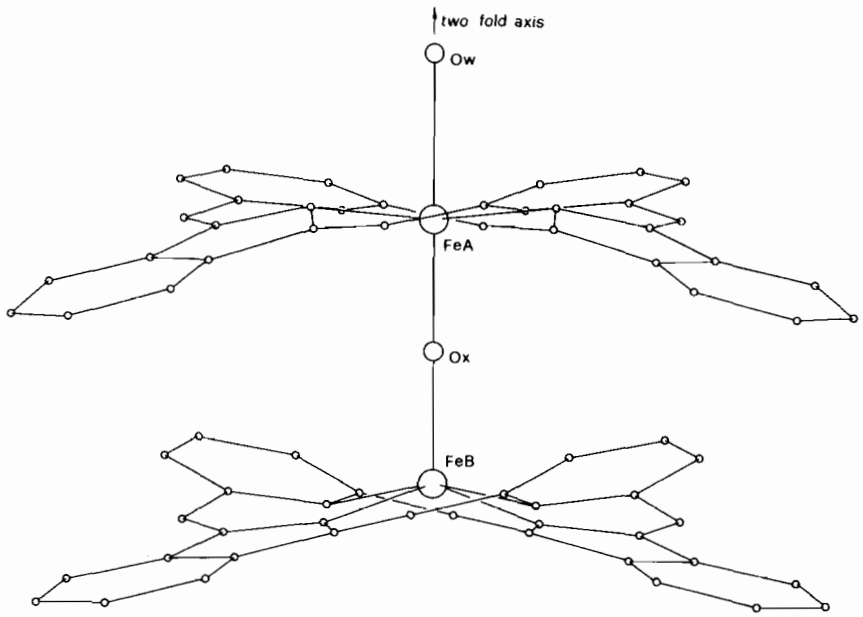

Fig. 3. Schematic view of the dimeric units, with the two-fold axis passing through the Ow–FeA–Ox–FeB atoms.

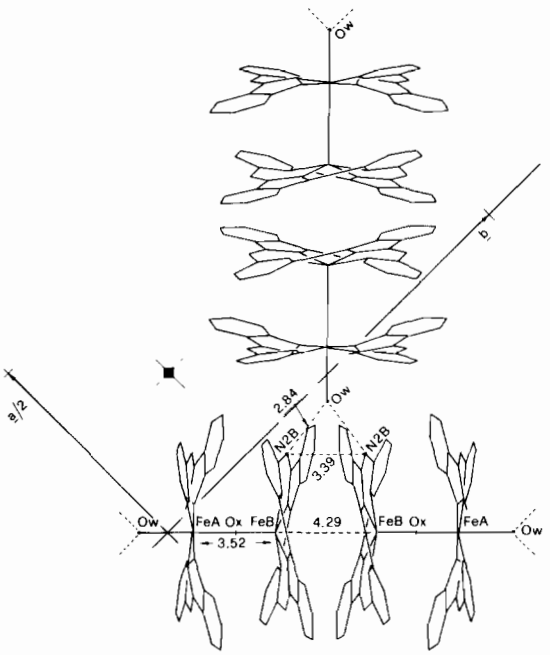

Fig. 4. Schematic view showing pairing of dimers into tetramers and the bidimensional hydrogen bond network.

The coordination about the two Fe atoms is not the same in the two crystallographically independent units. FeA lies in the plane of the four coordinated nitrogens, and a water molecule is coordinated *trans* to the oxo bridge (also lying on the two-fold axis), thus giving rise to hexacoordination. FeB is pentacoordinated and lies out of the hp plane by 0.45 Å, directly towards the bridging oxygen. The Fe–O_x distances are: FeA–O_x = 1.782(7) Å and FeB–O_x = 1.739(7) Å; the difference (0.043 Å) is presumably due to the different coordination about the Fe atoms. The axial distance FeA–O_w (2.210(9) Å) is longer than that found in the high-spin Fe(III) aquo complex Fe(III)TPP$(OH_2)_2^+$ (2.09 Å) [8]. The Fe–N-isoind(N1) and Fe–Npy(N3) distances are slightly longer in FeA (1.99, 2.21 Å) than in FeB (1.98, 2.18 Å).

Both macrocylic ligands in each crystallographically independent unit have a 'saddle' conformation, the planes of the isoindole rings being tilted by 15° in one direction and those of the pyridine rings by 11° in the opposite direction, with respect to the plane of the coordinated nitrogens. The C–C and C–N distances and ligand bond angles are comparable with those in other hemiporphyrazine complexes.

As shown in Fig. 4, the dimeric unit described is repeated via the symmetry operator $1/2 - x, -1/2 - y, z$ giving rise to a tetramer having the sequence O_w–FeA–O_x–FeB– – –FeB–O_x–FeA–O_w. The two dimers within the tetrameric units are rotated by 90° with respect to one other. The macrocycles coordinated to the FeB atoms thus face one another in such a way that the isoindole rings and the pyridine rings closely overlap. Thus, although the FeB–FeB distance is 4.29 Å, the average distance between the atoms of the two macrocycles is only 3.4 Å. Repetition of this tetramer via the four-fold axis passing through 1/4 1/4 z generates a two-dimensional net which develops perpendicular to the

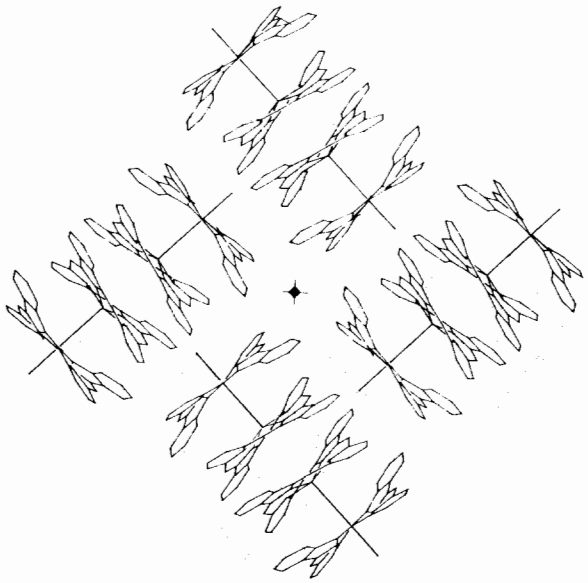

Fig. 5. Projection of the structure along the *c* direction.

crystallographic *c* axis. H-bonding interactions (2.84 Å) occur between the water coordinated to the FeA atoms of a tetramer and the nitrogens (N2B) of the two hemiporphyrazine groups coordinated to FeB of an adjacent tetramer (see Fig. 4).

Figure 5 shows the projection of the structure along the *c* axis. It is evident from this projection that channels between the external atoms of the macrocycles are formed running along the four-fold crystallographic axis. These channels are 'wavy', having a maximum diameter of 7 Å across the N2A atoms and 5.8 Å across the C9A atoms. The water of crystallisation lies in these channels and more or less in the same plane as the N2A atoms of the macrocycles.

Discussion

The crystal structure analysis demonstrates that the Fe–O–Fe bond in hpFe–O–Fehp–OH_2 is strictly linear. Such a linear arrangement is believed to be more favourable for transmitting exchange interactions via a π bonding mechanism because it allows maximum overlap of the two oxygen $p\pi$ orbitals with the metal $d\pi$ orbitals. The torsion angle of the two bridged Fehp units about the Fe–O–Fe bond is only 6°. A greater torsion angle is usually found in μ-oxo porphyrinate complexes (22.7–35.4°) [7, 9]. Presumably, such an eclipsed structure also favours greater $d\pi$(M)–$p\pi$(O)–$d\pi$(M) interaction [9].

There are no other structural data for pentacoordinated Fe(III)hp species with which the parameters obtained for the FeB$(N1B)_2(N3B)_2O$ group can be compared. However, we note that the FeB–N1B and FeB–N3B distances (1.981 and 2.180 Å, respectively) are more comparable to those found for high-spin Nihp$(py)_2$ (1.97 and 2.18 Å) [10] than to those for diamagnetic Nihp (1.863 and 1.998 Å) [11]. This is consistent with an occupied metal $3d_{x^2-y^2}$ orbital, *i.e.* with a high-spin Fe(III). The FeB–O_x (= 1.739 Å) and FeB–C_t (= 0.45 Å) distances are comparable to those in high-spin Fe μ-oxo dimers [12, 13]. In particular, the FeB–Ox distance is almost the same as the shortest Fe–Ox distance found (1.73 Å) in $[Fe(protoMe)]_2O$ [7]; this suggests a high bond order.

As expected, given the coplanarity of FeA with the four coordinated nitrogens, the macrocycle cavity shows a radial expansion: the FeA–N1 and FeA–N3 distances are slightly longer than those in the five-coordinate moiety, by a mean value 0.03 Å. This is also consistent with a high-spin state for the six-coordinate FeA. The different stereochemistry of the two Fe atoms is also reflected in the axial Fe–Ox distances: FeA–Ox (= 1.782(7) Å) is significantly higher than FeB–Ox (= 1.739(7) Å).

In agreement with an occupied dz^2 orbital for FeA, the axial FeA–O_w distance is long, 2.21 Å, indicating that the Fe(III)–OH_2 bond is weak. It is not possible to say how much this lengthening is due to the trans influence of the Fe–oxo moiety present, because of the lack of a model Fe(III)hp-$(H_2O)_2^+$ complex for comparison.

The thermal stability of the H_2O-μ-oxo adduct is probably due to the combined intramolecular H_2O–Fe and intermolecular OH_2–N interactions (see Fig. 4). Nevertheless, this adduct compound is less stable than the high-spin Fe(II)hp(H_2O), in which both kinds of H_2O interactions are also present [1]. In line with this lower H_2O– complex interaction, the ν_{OH} band in Fe(III) μ-oxo-hydrate lies at a higher energy level than the corresponding band in the Fe(II) hydrate.

Iron μ-oxo porphyrins containing additional peripheral ligands have not been reported previously. This has been ascribed to the marked shifting of the large iron ion out of the macrocycle plane towards the bridging oxygen [14]. This displacement has been attributed by different authors to various effects such as the structural rigidity of the macrocycle, the strong metal–oxo interaction and the non-bonding repulsion of the oxo ligand with the porphyrin core. Recently monomeric high-spin Fe(III) porphyrins have been reported to give hexacoordination with the Fe(III) lying in the macrocycle plane [8, 15].

Hemiporphyrazine is a virtually planar system having an asymmetric coordination cavity, with C_t N1 = 1.927 Å and C_t–N3 = 2.245 Å [16]. The average C_t–N (= 2.09 Å) is significantly larger than C_t–Npor (= 2.04 Å). This means that, compared with porphyrins, the hemiporphyrazine cavity can more readily accommodate high-spin ions in the plane. Co(II)hp(γ-pic)$_2$ [17] is an example; the Co(II) is high-spin and coplanar with the four bonding

TABLE III. Relevant Structural Parameters in Hemiporphyrazine Metal Complexes

	Nihp	$(FehpO)_n$	hpH_2	$Gehp(C_4H_9O_2)_2$	$Gehp(C_6H_9)_2$	$Nihppy_2$	$[(Fehp)_2]O·H_2O$
M–N isoind	1.863	1.91	1.927	1.934	1.956	1.97	1.985[a]
M–N py	1.998	2.135	2.245	2.175	2.172	2.18	2.195[a]
Ligand deviation α	25°	30°	5°	planar	7–9°	8–9°	11–15° [a]
$d_{x^2-y^2}$ occupation	0	0		2	2	1	1
Reference	11	2	16	21	22	10	this work

[a]Average value for the crystallographically independent FeAhp and FeBhp units of the dimer.

nitrogens of the macrocycle. Further, due to the relatively weak ligand field of the macrocycle, metallo-hemiporphyrazines tend to give axial coordination.

The cofacial orientation of two dimers (Fig. 4), analogous to the dimerisation observed in several five-coordinate porphyrins [18a–c] generates a tetramer. The mutual rotation of the dimers by 90°, to minimize steric interactions between the cofacial macrocycles, leads to a mean separation of 3.4 Å. This value is well within the range, 3.2–3.5 Å, generally recognized as indicating the presence of $\pi-\pi$ interactions [19]. Preliminary semi-empirical MO calculations [20] provide further evidence for the presence of this type of intermolecular interaction stabilising the pairing of the dimers into tetramers. On the other hand, intermolecular hydrogen bonding certainly plays a role in stabilising the solid state structure.

Antiferromagnetic coupling between the two high-spin Fe(III) ions of the μ-oxo dimers usually leads to μ_{eff} values (r.t.) in the range 1.5–2.0 BM [14a]. The value found for $[(Fehp)_2O]H_2O$ (= 2.02 BM) is close to the range. Note, however, that the structure of the compound indicates that several factors combine in favouring extensive overlap and hence large magnetic interactions.

As a final point, let us consider the 'saddle' deformation of the hemiporphyrazine macrocycle in this complex and in the others for which crystal structures have been described. A quantitative measure of this deformation is provided by the angle formed between the isoindole planes and the plane of the four internal nitrogens, α. (The pyridine planes are bent by about the same amount in the opposite direction.) The factors determining this angle are still obscure. Table III lists the M–Nisoind and M–Npy distances and the out-of-plane deviation of the ligand, α. From the few data available, it appears that the largest deviations from planarity for a reduced cavity occur due to relatively small metal ions having an empty $d_{x^2-y^2}$ orbital, *i.e.* Nihp and $(FehpO)_n$. This deviation is significantly lower when shortening of one bond is accompanied by a lengthening of the other bond. This occurs in complexes in which the metal ions are largest in terms of ionic radius or because of the presence of an occupied $d_{x^2-y^2}$ orbital.

References

1 I. Collamati, E. Cervone and R. Scoccia, *Inorg. Chim. Acta, 98*, 11 (1985).
2 W. Hiller, J. S. Strähle, A. Datz, M. Hanack, W. E. Hatfield, L. W. Haar and P. Gutlich, *J. Am. Chem. Soc., 106*, 329 (1984).
3 D. Attanasio, I. Collamati and E. Cervone, *Inorg. Chem., 22*, 3281 (1983).
4 B. N. Figgis and R. S. Nyholm, *J. Chem. Soc.*, 331 (1959).
5 'International Tables for X-ray Crystallography, Vol. IV', Kynoch Press, Birmingham, 1974.
6 G. M. Sheldrix, 'The SHELX Program System', University Chemical Laboratory, Cambridge, 1976.
7 J. T. Landrum, D. Grimmet, K. J. Haller, W. R. Scheidt and C. A. Reed, *J. Am. Chem. Soc., 103*, 2640 (1981) and refs. therein.
8 M. E. Kastner, W. R. Scheidt, T. Mashiko and C. A. Reed, *J. Am. Chem. Soc., 100*, 666 (1978).
9 (a) H. Masuda, T. Taga, K. Osaki, H. Sugimoto, M. Mori and H. Ogoshi, *J. Am. Chem. Soc., 103*, 2199 (1981); (b) J. P. Collman, C. E. Barnes, P. J. Brothers, T. J. Collins, T. Ozawa, J. C. Galluci and J. A. Ibers, *J. Am. Chem. Soc., 106*, 5151 (1984).
10 E. Agostinelli, D. Attanasio, I. Collamati and V. Fares, *Inorg. Chem., 23*, 1162 (1984).
11 J. C. Speakman, *Acta Crystallogr., 6*, 784 (1953).
12 W. R. Scheidt, in D. Dolphyn (ed.), 'The Porphyrins, Vol. III', Academic Press, New York, 1978, p. 484.
13 M. C. Weiss and V. L. Goedken, *Inorg. Chem., 18*, 819 (1979).
14 (a) W. I. White, in D. Dolphin (ed.), 'The Porphyrins, Vol. V', Academic Press, New York, 1979, p. 324; (b) D. Lancon and K. M. Kadish, *Inorg. Chem., 23*, 3942 (1984).
15 W. R. Scheidt, I. A. Cohen and M. E. Kastner, *Biochemistry, 18*, 3546 (1978); W. R. Scheidt, D. K. Geiger and K. J. Haller, *J. Am. Chem. Soc., 104*, 495 (1982).
16 E. C. Bissel, *Ph.D. Thesis*, (University Microfilms N 70-25) Case Western University, 1970.
17 G. Dessy and V. Fares, results to be published.
18 (a) H. Masuda, T. Taga, K. Osaki, H. Sugimoto, Z. I. Yoshida and H. Ogoshi, *Inorg. Chem., 19*, 950 (1980); (b) W. R. Scheidt, Y. J. Lee and K. Hatano, *J. Am. Chem. Soc., 106*, 3191 (1984); (c) W. R. Scheidt, D. K. Geiger and Y. J. Lee, 'Abstracts of XXIIIth ICCC', Boulder, Colo., 1984, p. 625.
19 F. H. Herbstein, *Perspect. Struct. Chem., 4*, 166 (1971).
20 M. Bossa, private communication.
21 H. J. Hecht and P. Luger, *Acta Crystallogr., Sect. B:, 30*, 2843 (1974).
22 W. Hiller, J. Strähle, K. Mitulla and M. Hanack, *Ann. Chem.*, 1946 (1980).